RSC Advances

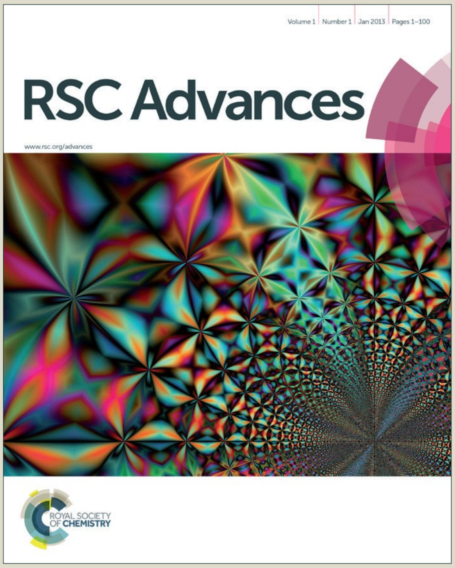

ROYAL SOCIETY
OF CHEMISTRY

www.rsc.org/advances

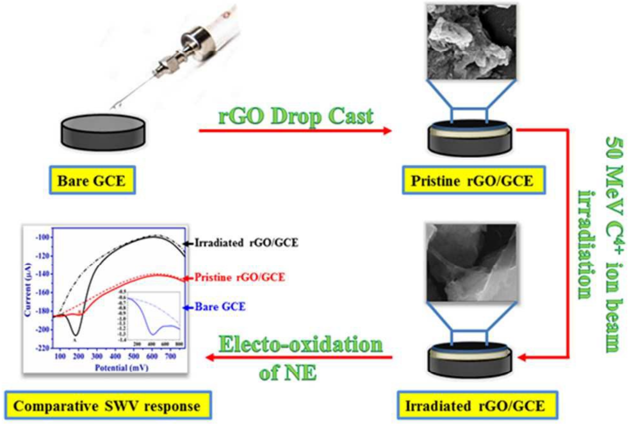

A high energy carbon ion beam irradiated sensor has been used for the sensitive determination of norepinephrine

254x190mm (96 x 96 DPI)

Structural and electrochemical characterization of carbon ion beam irradiated reduced graphene oxide and its application in voltammetric determination of Norepinephrine

Rosy*, Fouran Singh**, Rajendra N. Goyal*@

*Department of Chemistry, Indian Institute of Technology Roorkee, Roorkee -247 667 (India)
** Material Science Group, Inter University Accelerator Centre, Aruna Asif Ali Marg, New Delhi – 110 067 (India)
@E.Mail: rngcyfcy@iitr.ac.in; Tel +91-1332-285794 (O)

Abstract

Irradiation of reduced graphene oxide (rGO) sheets using 50 MeV C^{4+} ion beam has been implemented to create disorders. The changes in the charge transfer resistance (R_{CT}) and structural variations in rGO upon irradiation have been studied using electrochemical impedance spectroscopy (EIS), Raman spectroscopy and field emission scanning electron microscopy (FE-SEM). Irradiation of rGO with 50 MeV C^{4+} ion beam resulted in three fold decreased charge transfer resistance (R_{CT} 32.91 Ω) in comparison to 93.42 Ω corresponding to pristine rGO. Electrochemical properties of irradiated rGO have been further investigated by developing an irradiated rGO modified glassy carbon electrode (GCE) for the analysis of norepinephrine (NE). Voltammetric experiments showed that irradiated rGO modified GCE (Irradiated rGO/GCE) exhibited superior response towards NE oxidation in comparison to both the pristine rGO/GCE and bare GCE. Thus, NE has been quantified using Irradiated rGO/GCE in a linear concentration range of 1 – 200 μM with a detection limit of 50 nM. Detection sensitivities corresponding to bare, pristine rGO and irradiated rGO modified GCE were 0.0173, 0.1335 and 0.769 $\mu A\ \mu M^{-1}$ respectively, demonstrating substantial improvement in sensing and electrocatalytic behaviour of rGO on exposure to ion beam. To ensure the analytical applicability of the fabricated sensor it has been successfully applied for the estimation of norepinephrine (NE) in injection, human urine and serum samples and recovery >93 % with R.S.D < 3.5 % were achieved.

Keywords

Ion beam, reduced graphene oxide, voltammetry, Norepinephrine, Raman spectroscopy, electrochemical impedance spectroscopy

1. Introduction

Graphene has emerged as a subject of interest for a plethora of scientific disciplines due to its peculiar electron transport properties, high surface area, and chemical and mechanical stability [1,2]. Substantial efforts have been made in the inquisition of its electrochemical properties in the last era of scientific research, where global innovations in using graphene as a potential electrode material and its application in sensing and energy related devices have been widely documented [2-7]. Since, graphene has already outperformed in various technological and application based fields, like in fabrication of energy storage devices [8,9], its use as surface modification [5-7] and its execution as a substrate for sensing and energy production [10,11], the next leg of research in graphene lies in tailoring its exceptional and superior properties, by introducing defects using ion beams, chemical modification, or by means of doping [3,12]. Controlled insertion of defects in the graphene can be achieved in order to induce modification in its chemical, physical and mechanical properties [13]. As the presence of defects in graphene strongly affects the band gap and electronic transport properties, the study of defects, impurities and topographical changes in the graphene structure has been a pioneering topic of importance for both basic science and applied technology [14]. Last decade has seen ion irradiation as a useful method to produce disorder in carbon nanostructures like carbon nanotubes, fullerenes and graphene, because it allows tuneable ion energy, ion fluence etc. The graphene properties can be tailored from a highly conducting nano-crystalline graphene structures to poorly conducting amorphous carbon using optimized ion radiations [12,15,16]. As any damage or disorder created in the primitive sp^2 structure leads to reorganization of lattice arrangement around the defects, it results in alteration of many characteristic properties like electronic band structure, electron phonon scattering, carrier density, surface area, roughness etc. [13,17, 18].

Many approaches for the modification of graphene using ion beams have been reported in the last decade [13-17], but the execution of the modified graphene in analysis has limited exposure and thus, it has been considered worthwhile to investigate the effect of irradiation on the electrochemical and electro-catalytic properties of graphene. In the present paper, use of carbon ion beam for manipulating electronic properties of reduced graphene oxide (rGO) has been described followed by its characterization and application for the voltammetric analysis of Norepinephrine (NE), an important biomolecule belonging to the class of catecholamines. NE serves multiple functions in central nervous system and any alteration in its blood plasma concentration is associated with many pathological conditions like neurological diseases, cardiovascular problems, misbalance in muscle and tissue control etc. hence, its quantitative analysis has been a topic of intensive research in analytical and pathological sciences. In recent years, many sensors has been developed for NE quantification using different surface modifications and electrodes like carbon nanotubes paste electrode [19-21], composite of molecularly imprinted polymer [22], graphene modified electrodes [23,24] poly(glutamic acid) modified carbon paste electrode [25], MWNTs-ZnO/chitosan composites modified screen-printed electrode [26]. Thus, to provide an apt comparison, a sensor has been developed using the irradiated rGO for NE analysis and its practical application in assaying NE in complex biological fluids and pharmaceutical formulation has been presented.

2. Experimental

2.1 Reagents and chemicals

Analytical grade NE, uric acid (UA), xanthine (X) and hypoxanthine (HX) were acquired from Sigma Aldrich, USA. Reduced graphene oxide (rGO) was synthesized according to the previously reported method [23]. Phosphate buffers in the pH range of 2.0 to 11.0 (μ = 1 mol/L) were prepared following the method of Christian and Purdy [27]. Noradrenaline bitartrate injection (Neon Labs. Ltd.; Mumbai, Maharashtra, India) was obtained from the hospital of the Indian Institute of Technology Roorkee. All other chemicals and solvents used throughout the experimental determination were of reagent grade.

2.2 Instrumentation

All electroanalytical experiments were performed using a Bioanalytical voltammetric analyzer CV-50W (BAS; West Lafayette, USA) equipped with three electrodes, single compartment voltammetric cell. Glassy carbon electrode (GCE) was used as a working electrode along with Ag/AgCl (3M NaCl; BAS Model MF-2052 RB-5B) and platinum wire as reference and auxillary electrodes respectively.

Irradiation of rGO modified GCE was performed using 15 UD Pelletron Accelerator at Inter University Accelerator Centre, New Delhi, India. The effects of irradiation on the modified GCE were analyzed using FE-SEM (Field Emission Scanning Electron Microscopy; Zeiss ultra plus 55) and Raman spectroscopy (Renishaw invia Raman microscopy). Charge transfer resistance was calculated using Electrochemical impedance spectroscopy (EIS) performed on Versa Stat 3 galvanostat (PAR).

2.3 Preparation of modified electrode

Prior to modification, 1 cm^2 piece of GCE was mechanically polished with alumina slurry on a micro-cloth pad and rinsed thoroughly with double distilled water. 1 mg of rGO was then ultrasonically dispersed in 1 mL of dimethyl formamide (DMF). The reason for selecting DMF for making rGO dispersion was its large stability time in comparison to other organic solvents like chloroform, hexane or ethanol. Moreover, it is also reported in the literature that almost full exfoliation of graphite oxide into individual graphene oxide sheets is generally achieved in DMF [28]. Optimized volume of this rGO dispersion (20 μL) was then placed on the pre cleaned piece of GCE and kept undisturbed at room temperature for solvent evaporation. rGO modified GCE, was then exposed to a 50 MeV beam of carbon ions (C^{4+}) at different fluences ranging from 10^{11} to 10^{14} ions cm^{-2} with 15 UD Pelletron accelerator in the vacuum chamber, kept at a pressure of ~5 × 10^{-6} Torr. The irradiated piece of rGO modified GCE was the final sensing surface and the sensor was prepared by connecting it to a copper strip in order to provide electrical connection, which was then enclosed in the pocket between two scotch tapes having a hole of 3 mm on the front side for the exposure of electroactive surface to the test solution. The graphical representation of the detailed protocol followed for the electrode preparation has been demonstrated in Figure 1.

Figure 1 here

2.4 Sample preparations and voltammetric procedure

Stock solution of NE (1 mM) was prepared by dissolving the required amount of norepinephrine bitartrate monohydrate in double distilled water. Calibration standards (4 mL) in the concentration range of 1 to 200 μM were then prepared by adding required volume of stock solution to the test tube containing 2 mL of pH 7.2 phosphate buffer as supporting electrolyte and the final volume was made to 4 mL using double distilled water. Voltammograms were then recorded using following optimized parameters: initial potential (E_i): 0 mV, final potential (E_f): 600 mV, square wave amplitude: 25 mV, potential step: 4 mV and square wave frequency (f): 15 Hz.

2.5 Biological sample preparations

In spite of our best efforts, we were unable to find the biological samples of patients undergoing treatment with NE or those suffering from disorders resulting in abnormal NE level. Hence, for the investigation of NE in the real sample, urine and serum samples of healthy volunteers (1 male; age 27 and 1 female; age 25) were obtained from the hospital of I.I.T. Roorkee. Recovery studies were performed by spiking a known amount of NE in the filtered urine samples which were then diluted 3 times prior to analysis. Similarly, serum samples spiked with NE were diluted 5 times with pH 7.2 phosphate buffer in order to reduce matrix complexity.

3. Results and discussion

3.1 Characterization of irradiated sample

Figure 2 depicts the results of galvanostat impedance carried out at following parameters: AC start frequency (Hz): 10000, AC end frequency (Hz): 1, Amplitude (µA RMS): 100, points per decade: 10. From the Figure 2, it can be evidenced that irradiation at a fluence of 10^{12} ions cm^{-2} resulted in lower R_{CT} in comparison to pristine rGO. Whereas, rGO irradiated with ion fluence of 10^{14} ions cm^{-2} resulted in maximum R_{CT} and lowest capacitance as can be observed from Table 1. The rGO irradiated with fluence of 10^{11} ions cm^{-2} showed a R_{CT} in between that of pristine and rGO exposed to ion fluence of 10^{12} ions cm^{-2}, whereas, irradiation with 10^{13} ions cm^{-2} exhibited R_{CT} greater than pristine (Table 1). From the results, it can be seen that on increasing the ion fluence, number of vacancies or defects in rGO increases. However, irradiation at high fluence lead to increased number of defects, but, at the same time, it also resulted in damaged graphene lattices and more amorphous carbon [14,16] that can be seen in terms of higher R_{CT} for rGO irradiated at a fluence > 10^{12} ions/cm^2, as shown in Table 1. The increase in number of defects also increases the number of carriers and results in altered electronic structure of rGO, or to be specific, results in the formation of mid gap. The formation of the mid gap introduces a metallic regime in the electronic structure of rGO, which leads to enhanced conductivity. On the other hand, higher number of defects (beyond a certain limit) results in scattering centres, which hinders the mobility and reduces the conductivity of the graphene [12]. Hence, optimized ion fluence is required to get the desired results and thus, rGO irradiated with carbon ion beam at fluence 10^{12} ions/cm^2 is used for further investigations.

Raman spectroscopy is considered as the first choice for the study of carbon materials. It is a technique of excellence for the analysis of any change in hybridization or disorder present in the primitive structure of these materials [14]. Apart from being sensitive to defects, a Raman spectrum delivers much more information like length, thickness, doping etc. through altered intensities of various bands present in the corresponding Raman spectra [29]. Fig. 3 represents the characteristic Raman spectra of graphene having majorly 3 bands: a disorder induced D band (~1350 cm^{-1}), G band (~1600 cm^{-1}) and 2D band (~2700 cm^{-1}). From the figure, it can be seen that exposure to carbon ion beam at a fluence of 10^{12} ions cm^{-2} leads to increased intensity and increased wave length (red shift) of all the three bands present in the spectrum. The increased intensity of the D band symbolizes the presence of disorder or defect in the rGO structure, whereas, the increased I_D/I_G ratio of irradiated graphene indicates thinning of the reduced graphene oxide sheets as well as it is representing the increased number of defects in the rGO layers. This results into more number of layers exhibiting graphene like behaviour which can also be concluded from the decreased wavelength of G and D bands [14, 13, 29]. The thinning of rGO sheets can also be observed in the FE-SEM images as showed in Fig. 4, where, thin sheets of rGO can be seen in Fig 4(A), residing in between the two flakes, on the other hand, large and irregular rGO flakes were found to be scattered in the case of pristine rGO (Fig 4(B)).

Figure 2, 3, 4 and Table 1 here

3.2 Square wave voltammetry

To evaluate the effect of irradiation on the electrochemical properties of rGO towards NE oxidation, square wave voltammograms were recorded in 50 µM solution using bare, pristine rGO modified and irradiated rGO modified GCE. A well-defined oxidation peak at ~ 210 mV was observed in all the voltammograms corresponding to bare (GCE), pristine rGO/GCE, irradiated rGO/GCE respectively. A comparison of the voltammograms observed for NE at pristine and irradiated rGO is presented in Fig. 5. It can be seen that irradiation caused enhancement in the peak current and reduction of NE occurred at much lower potential (~ 180 mV) as compared to the pristine rGO, where, small peak at Ep ~ 210 mV was observed. At bare GCE, a well-defined peak for NE was observed at much higher potential (Ep ~ 400 mV), with approximately 50 times lower peak current in comparison to the current observed at irradiated rGO. Thus, it can be concluded that irradiation leads to efficient defect production and morphological changes in rGO, which showed electrocatalytic behavior and enhances the electron transport. Hence, all the further voltammetric studies involved throughout the experimental determination were carried out using irradiated rGO/GCE.

Fig 5 Here

3.2.1 Effect of pH

The effect of pH on the oxidation peak potential and peak current of NE was analyzed in the pH range of 2.0 – 11.0 using irradiated rGO/GCE. It was witnessed that with increasing pH, the oxidation potential of NE shifted to less positive values. The dependence of Ep on pH was linear and can be documented using the equation:

$$\text{Ep (mV vs. Ag/AgCl)} = -52.40\ \text{pH} + 564.38\ (R^2 = 0.9975)$$

The slope having a value close to ~ 59 mV/pH, indicated that the oxidation of NE proceeded by involving equal number of electrons and protons.

3.2.2 Effect of concentration

To examine the effect of NE concentration on the oxidation peak current, voltammograms were recorded at different concentrations ranging from 1 to 200 μM at bare GCE, pristine rGO and irradiated rGO modified GC electrodes. At all the three electrodes the peak current was found to increase with increasing concentration of NE, as showed in Fig. 6. The dependence of Ep on concentration has been presented in the inset of Fig. 6 and can be expressed by the following equations:

$$i_p\ (\mu A) = 0.0173\ [\text{NE}\ (10\text{-}200\mu M)] - 0.2768\quad (R^2 = 0.987)\qquad \text{: Bare GCE}$$

$$i_p\ (\mu A) = 0.1335\ [\text{NE}\ (5\text{-}200\mu M)] + 3.8721\quad (R^2 = 0.989)\qquad \text{: pristine rGO /GCE}$$

$$i_p\ (\mu A) = 0.769\ [\text{NE}\ (1\text{-}200\ \mu M)] + 10.162\quad (R^2 = 0.991)\qquad \text{: Irradiated- rGO/GCE}$$

From the slopes of the three equations, it can be seen that exposing rGO to carbon ion beam leads to ~ 6 fold increase in the sensitivity in comparison to pristine rGO. It was observed that the value of the detection limit (50 nM) at irradiated rGO/GCE was much lower in comparison to 1.29 μM corresponding to pristine rGO/GCE. The detection limit is calculated by using 3σ/b where 'σ' is the standard deviation of three blank runs recorded in phosphate buffer (pH 7.2) using the respective sensor and 'b' symbolizes the slope of calibration plot.

Figure 6 Here

3.2.3 Effect of frequency

The nature of the electrode process was evaluated by recording SW voltammograms for 50 μM NE at frequencies ranging from 5 to 100 Hz. An increase in the peak current with increasing frequency was observed and it was found that the peak current varies linearly with the square root of frequency, suggesting that the oxidation of NE at irradiated sensor followed a diffusion controlled process [23].

3.2.4 Interference Study

To establish the practical utility of the fabricated sensor, it was necessary to check the interference of commonly found biomolecules in blood and urine, like uric acid (UA), ascorbic acid (AA), xanthine (X) and hypoxanthine (HX). To evaluate the interference (if any) of these biomolecules on the peak current of NE, SW voltammograms were recorded in a solution having a fixed concentration of NE (1 μM) and increasing concentration of other biomolecules like UA, AA, X and HX. Fig. 7 demonstrates a successful application of the present protocol in analyzing NE at irradiated rGO modified GCE, as it can be seen from the figure, that the well-defined and well-separated peaks at 310, 670 and 1050 mV corresponding to UA, X, and HX respectively were obtained along with NE oxidation peak at 200 mV. AA exhibited a peak at -130 mV and thus has not been shown in Fig 7. It can further be seen that no substantial change in the peak current or peak potential of NE was observed with the increasing concentration of other biomolecules and hence, the present sensor can be applied for assaying NE in biological fluids.

Figure 7 here

4. Analytical applicability

4.1 Analysis of pharmaceutical preparation

The performance of irradiated rGO/GCE sensor was also evaluated for the determination of NE content in Noradrenaline bitartrate injection (Neon Labs. Ltd.; Mumbai, Maharashtra, India). The required amount of the injection volume was diluted to bring the concentration of NE in the concentration range of the standard calibration plot. SW voltammograms were then recorded and a well-defined peak for NE oxidation was observed at ~180 mV. The NE content in the injection sample was then estimated using the proposed method. The experimentally detected value and labeled value are compared in Table 2. It can be seen that the calculated value is in good agreement with the claimed value of NE with a relative standard deviation of ± 0.7 % (n=3). Therefore, it is recommended that the fabricated sensor can be applied for assaying NE in pharmaceutical formulation analysis.

Table 2 here

4.2 Analysis of human urine and serum

The practical utility of the present sensor was also evaluated by applying it for the detection of NE in biological fluids like human urine and serum. No peak for NE was observed in the filtered urine sample of healthy volunteer, as NE concentration discharged in healthy human is very low [30]. Hence, to carry out recovery studies, standard addition method was followed. A known amount of NE stock solution was spiked into the filtered urine and serum sample which were then diluted three and five times respectively with pH 7.2, phosphate buffer. The solutions thus obtained were further diluted for the preparation of test solutions having different concentrations and voltammograms were then recorded. The concentration of NE was then back calculated by inserting the observed peak current in the regression equation of the calibration plot. The observed and spiked values of NE are compared in Table 3 and it can be seen that recovery > 93% was witnessed in both serum and urine samples. Hence, the present sensor can be successfully invoked for practical determination of NE in biological fluids.

Table 3 Here

5. Reproducibility and stability

The reproducibility of the irradiated rGO/GCE sensor was estimated by recording five consecutive SW voltammograms in 50 μM NE solution. The oxidation peak current corresponding to 5 voltammograms showed a R.S.D of 3.7 % which demonstrated efficient reproducibility of the sensor. Stability of modification protocol was also studied by storing the modified sensor at room temperature for 15 days and recording voltammograms regularly. Even after 15 days, 91.4 % of the original oxidation peak current was witnessed which indicated an excellent stability of the modification.

6. Conclusion

The application of ion beam irradiation for manipulating chemical and physical properties of rGO has been investigated in the present manuscript. It has been observed that irradiation lead to thinning of rGO sheets and decreased charge transfer resistance. The application of the irradiated rGO sensor has been extended for monitoring the electrochemical oxidation of NE in biological samples. The ability of irradiated rGO modified GCE for the voltammetric estimation of NE has been compared with the pristine rGO modified GCE and bare GCE, and it has been observed that the irradiated rGO catalyse the oxidation of NE and enhanced sensitivity and selectivity is observed. A well-defined, intense oxidation peak corresponding to NE was observed at 180 mV using Irradiated rGO/GCE. A detection limit of

50 nM is observed for the present protocol which is much lower in comparison to bare GCE (4.53 μM), pristine rGO/GCE (1.29 μM) as well as many other reported sensors for NE in recent years and is presented in Table 4. This study suggested the need for much more intense investigations for development of sensors, which can serve mankind by easing analytical determinations of important biomolecules for fast medical diagnosis.

Table 4 here

5 Acknowledgement

One of the **a**uthors (Rosy) is thankful to the Ministry of Human Resources Development, New Delhi for the award of Senior Research Fellowship. Thanks are also due to Director, Inter University Accelerator Centre, New Delhi for permitting irradiation experiments.

References

[1] D. A. C. Brownson, C. W. Foster, Craig E. Banks, *Analyst*, 2012, **137**, 1815-1823.

[2] T. Gan, S. Hu, *Microchim. Acta*, 2011, **175**, 1-19.

[3] D. A. C. Brownson, C. E. Banks, *Analyst*, 2010, **135**, 2768-2778.

[4] K. R. Ratinac, W. Yang, J. J. Gooding, P. Thordarson, F. Braet, *Electroanalysis*, 2011, **23**, 803-826.

[5] P. Gupta, S. K. Yadav, B. Agrawal, R. N. Goyal, *Sens. Actuators B*, 2014, **204**, 791–798.

[6] M. Purushotham, P. Gupta, R. N. Goyal, *Talanta*, 2015, **143**, 328–334.

[7] P. Gupta, R. N. Goyal, *RSC Adv.*, 2015, **5**, 40444–40454.

[8] R. Raccichini, A. Varzi, S. Passerini, B. Scrosati, *Nat. Mater.*, 2015, **14**, 271–279.

[9] N. Mahmood, C. Zhang, H. Yin, Y. Hou, *J. Mater. Chem. A*, 2014, **2**, 15–32.

[10] R. Ramachandran, V. Mani, S.-M. Chen, R. Saraswathi, B.-S. Lou, *Int. J. Electrochem. Sci.*, 2013, **8**, 11680 – 11694.

[11] G. Jo, M. Choe, S. Lee, W. Park, Y. H. Kahng, T. Lee, *Nanotechnology*, 2012, **23**, 112001 (19pp).

[12] S. H. M. Jafri, K. Carva, E. Widenkvist, T. Blom, B. Sanyal, J. Fransson, O. Eriksson, U. Jansson, H. Grennberg, O. Karis, R. A. Quinlan, B. C. Holloway, K. Leifer, *J. Phys. D: Appl. Phys.*, 2010, **43**, 045404 (8pp).

[13] G. Compagnini, F. Giannazzo, S. Sonde, V. Raineri, E. Rimini, *Carbon*, 2009, **47**, 3201–3207.

[14] G. Compagnini, G. Forte, F. Giannazzo, V. Raineri, A. L. Magna, I. Deretzis, *J. Mol. Struct.*, 2011, **993**, 506–509.

[15] E. H. Ahlgren, J. Kotakoski, O. Lehtinen, A. V. Krasheninnikov, *Appl. Phys. Lett.*, 2012, **100**, 233108 .

[16] M.-J. Jung, M.-S. Park, Y.-S. Lee, *J. Nanomater.*, 2015, 240264 (8 pp) http://dx.doi.org/10.1155/2015/240264.

[17] C. Deng, W. Lin, S. Eimer, D. Ravelosona, C. Chappert, W. Zhao, Proceedings of the 13th IEEE International Conference on Nanotechnology Beijing, China, August 5-8, 2013.

[18] A. V. Krasheninnikov, F. Banhart, *Nat. Mater.*, 2007, **6**, 723 – 733.

[19] M. Ansari, S. Kazemi, M. A. Khalilzadeh, H. Karimi-Maleh, Md. B. P. Zanousi, *Int. J. Electrochem. Sci.*, 2013, **8**, 1938 – 1948.

[20] H. Beitollahi, S. Mohammadi, *Mater. Sci. Eng. C*, 2013, **33**, 3214–3219.

[21] S. Salmanpour, T. Tavana, A. Pahlavan, Md. A. Khalilzadeh, A. A. Ensafi, H. Karimi-Maleh, H. Beitollahi, E. Kowsari, D. Zareyee, *Mater. Sci. Eng. C*, 2012, **32**, 1912–1918.

[22] J. Chen, H. Huang, Y. Zeng, H. Tang, L. Li, *Biosens. Bioelectron.*, 2015, **65**, 366–374.

[23] Rosy, S. K. Yadav, B. Agrawal, M. Oyama, R. N. Goyal, *Electrochim. Acta*, 2014, **125** , 622–629.

[24] X. Ma, M. Chen, X. Li, A. Purushothaman, F. Li, Int. *J. Electrochem. Sci.*, 2012, **7**, 991 – 1000.

[25] P.S. Ganesh, B.E. Kumara Swamy, *J. Electroanal. Chem.*, 2015, **752**, 17–24.

[26] Y. Wang, S. Wang, L. Tao, Q. Min, J. Xiang, Q. Wang, J. Xie, Y. Yue, S. Wu, X. Li, H. Ding, *Biosens. Bioelectron.*, 2015, **65**, 31–38.

[27] G. D. Christian, W. C. Purdy, *J. Electroanal. Chem.*, 1962, **3**, 363-367.

[28] J. I. Paredes, S. Villar-Rodil, A. Martınez-Alonso, J. M. D. Tascon, *Langmuir*, 2008, **24**, 10560-10564.

[29] I. Childres, L. A. Jauregui, W. Park, H. Cao, Y. P. Chen, Raman spectroscopy of graphene and related materials, Nova Science publishers, USA, 2012.

[30] F. C. Luft, L. I. Rankin, D. P. Henry, R. Bloch, C. E. Grim, A. E. Weyman, R. H. Murray, M. H. Weinberger, *Hypertension*, 1979, **1**, 261- 266.

Table 1: Values of Charge Transfer Resistance (R_{CT}) and Capacitance obtained from circuit fit in impedance corresponding to pristine rGO and rGO irradiated at different ion fluences.

Parameter	**pristine**	**Irradiation with ion fluence / ions cm^{-2}** **10^{11}**	**10^{12}**	**10^{13}**	**10^{14}**
R_{CT} (Ω)	93.42	80.97	32.91	110.8	187.1
Capacitance (μF)	3.616	3.892	6.284	2.592	1.157

Table 2. The determination of NE in pharmaceutical injection using carbon ion irradiated rGO modified GCE sensor.

Sample	**Used amount (μM)**	**Detected amount (μM)**	**Error %**
Noradrenaline bitartrate	31.32	31.37	0.1600

*The R.S.D. value for determination was 0.77% for n = 3

Table 3: Recovery experiments of NE in human urine and serum samples of healthy volunteers using Carbon ion Irradiated rGO /GCE voltammetric sensor

Amount added (µM)	Amount detected (µM)	Recovery (%)
URINE		
Sample 1		
10	09.72	97.20
25	25.16	100.6
50	49.83	99.66
Sample 2		
50	49.13	98.26
75	74.79	99.72
100	99.47	99.47
BLOOD SERUM		
Sample 1		
25	24.76	99.04
50	50.48	100.9
75	73.69	98.25
Sample 2		
10	09.34	93.40
50	49.62	99.24
100	98.27	98.27

*The R.S.D. value for determination was less than 3.18% for urine and 2.77% for serum respectively for n = 3

Table 4: Comparison of the detection limits and recovery studies performed at Carbon ion Irradiated rGO /GCE with other recently reported sensors.

Ref.	Method/ Modification	L.O.D/nM	Recovery
[19]	MBIDZCl/MWCNT/CPE	80	Urine, Plasma
[20]	5-mino-3′,4′-dimethyl-biphenyl-2-ol/CPE	590	plasma
[21]	MWCNTs/CarbonIonicLiquidElectrode	90	Urine, Plasma
[22]	MIP-coated PdNPs/GCE	100	Urine
[23]	rGO /Pd electrode	67.4	Urine
[24]	Graphene/GCE	400	No
[25]	poly(glutamic acid)/CPE	430	No
[26]	MWNTs-ZnO/chitosan SPE	200	Rat CSF
This Work	Carbon ion Irradiated rGO /GCE	50	Urine, Plasma

*MBIDZCl: 1-methyl-3-butylimidazolium chloride, CPE: carbon paste electrode, GCE: Glassy carbon electrode, rGO: Reduced Graphene oxide, SPE: Screen printed electrode, CSF: cerebrospinal fluid

Figure captions

Figure 1: Graphical demonstration of the modification steps involved in the preparation of sensor.

Figure 2: Electrochemical impedance spectra corresponding to (A) carbon ion irradiated rGO and (B) pristine rGO recorded in 5 mM $K_3[Fe(CN)_6]$ and 1M KCl.

Figure 3: Raman spectra corresponding to rGO and Carbon ion irradiated rGO.

Figure 4: Typical FE-SEM images of (A) Carbon ion irradiated rGO and (B) pristine rGO.

Figure 5: Comparitive Square wave voltammogram recorded in 50 µM NE using (A) carbon ion irradiated and (B) pristine rGO modified GCE. Inset is the voltammetric response of 50 µM NE corresponding to bare GCE

Figure 6: Square wave voltammograms recorded at (a) 1 µM, (b) 10 µM, (c) 25 µM, (d) 50 µM, (e) 75 µM, (f) 100 µM and (g) 200 µM NE concentration using carbon ion irradiated rGO modified GCE. Inset is the calibration curve corresponding to (a') carbon ion irradiated graphene modified GCE (b') pristine graphene modified GCE and (c') bare GCE.

Figure 7: Square wave voltammograms observed for a solution containing (a) 10 µM UA + 1 µM NE + 10 µM X + 10 µM HX (b) 25 µM UA+ 1 µM NE + 25 µM X + 25 µM HX (c) 60 µM UA+ 1 µM NE + 60 µM X + 25 µM HX. Background is represented by dotted line.

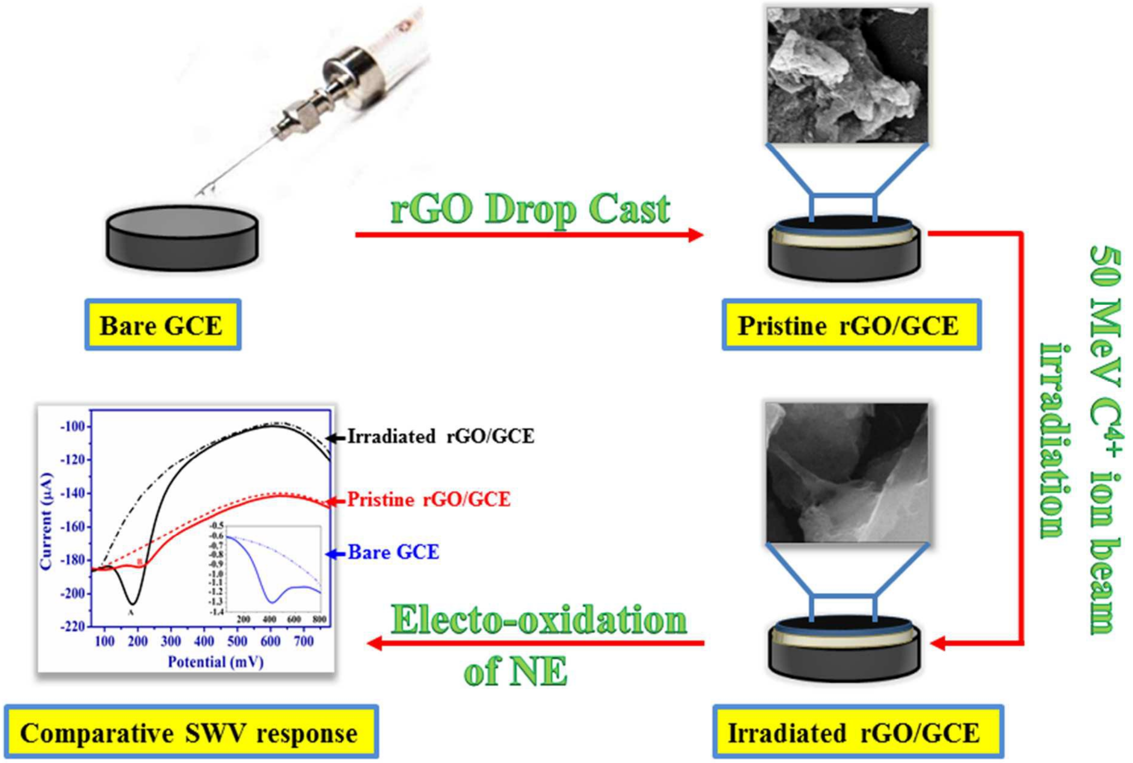
rGO Drop Cast
Bare GCE
Pristine rGO/GCE
50 MeV C4+ ion beam irradiation
Irradiated rGO/GCE
Electo-oxidation of NE
Comparative SWV response
Irradiated rGO/GCE
Pristine rGO/GCE
Bare GCE
Current (µA)
-100
-120
-140
-160
-180
-200
-220
Potential (mV)
100
200
300
400
500
600
700
A
B
-0.5
-0.6
-0.7
-0.8
-0.9
-1.0
-1.1
-1.2
-1.3
-1.4
200
400
600
800

Figure 1

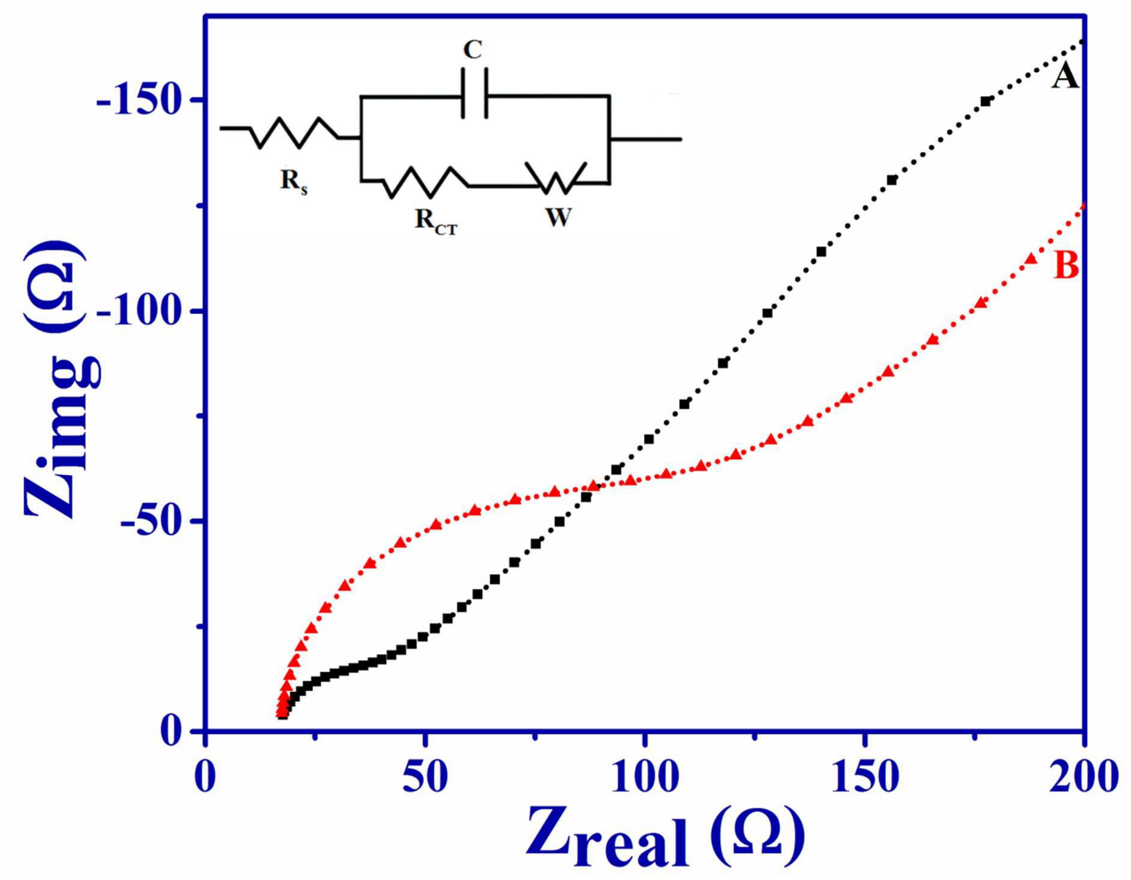

Figure 2

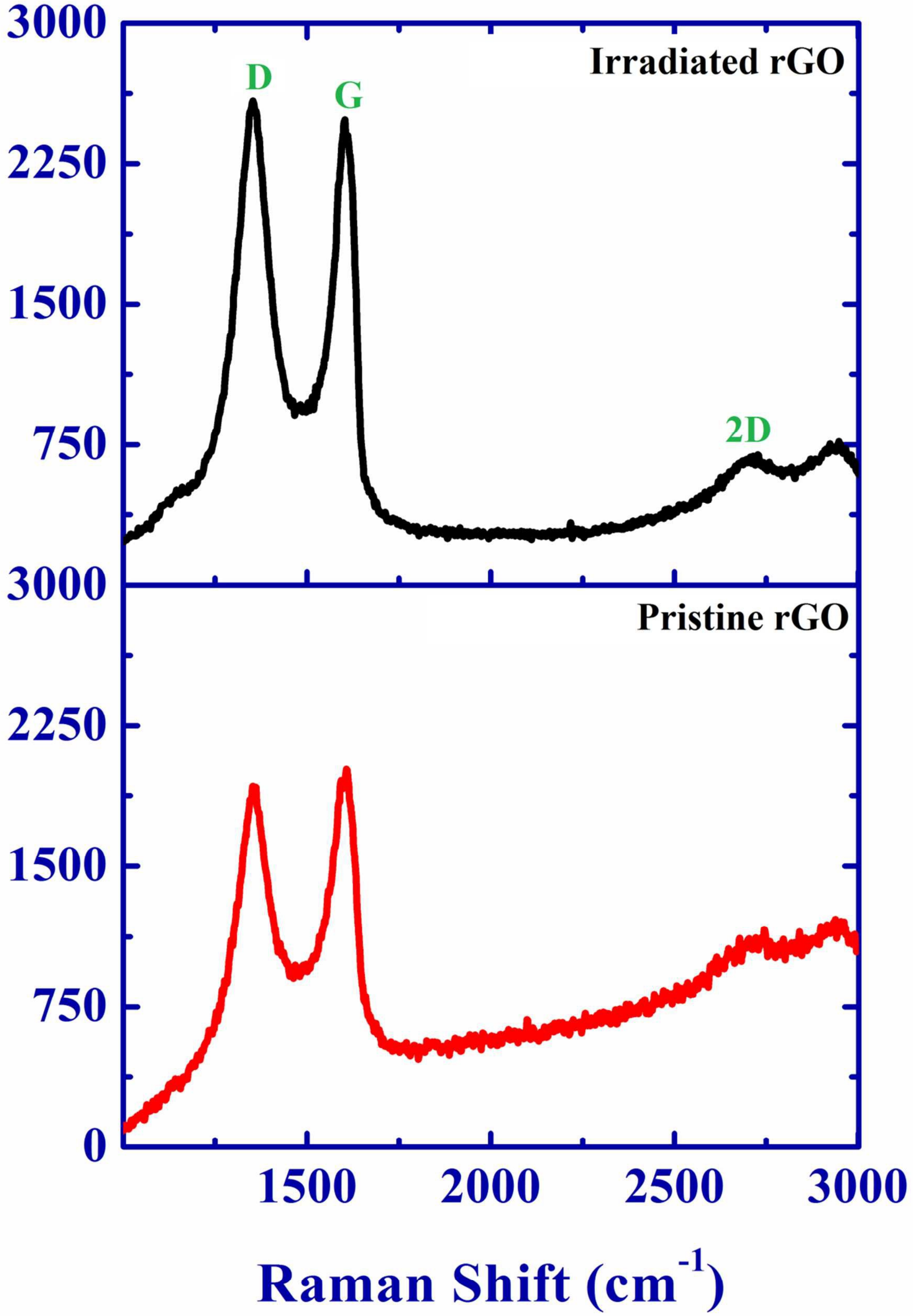
3000
2250
1500
750
3000
2250
1500
750
0
Irradiated rGO
D
G
2D
Pristine rGO
1500
2000
2500
3000
Raman Shift (cm^{-1})

Figure 3

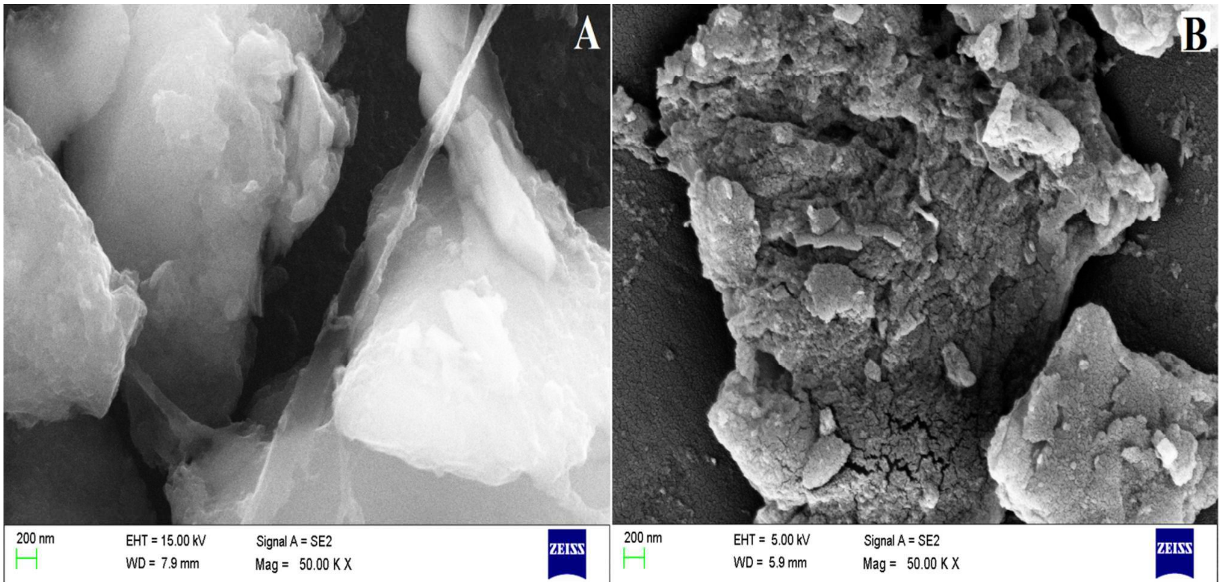
A
B
200 nm
EHT = 15.00 kV
WD = 7.9 mm
Signal A = SE2
Mag = 50.00 K X
200 nm
EHT = 5.00 kV
WD = 5.9 mm
Signal A = SE2
Mag = 50.00 K X

Figure 4

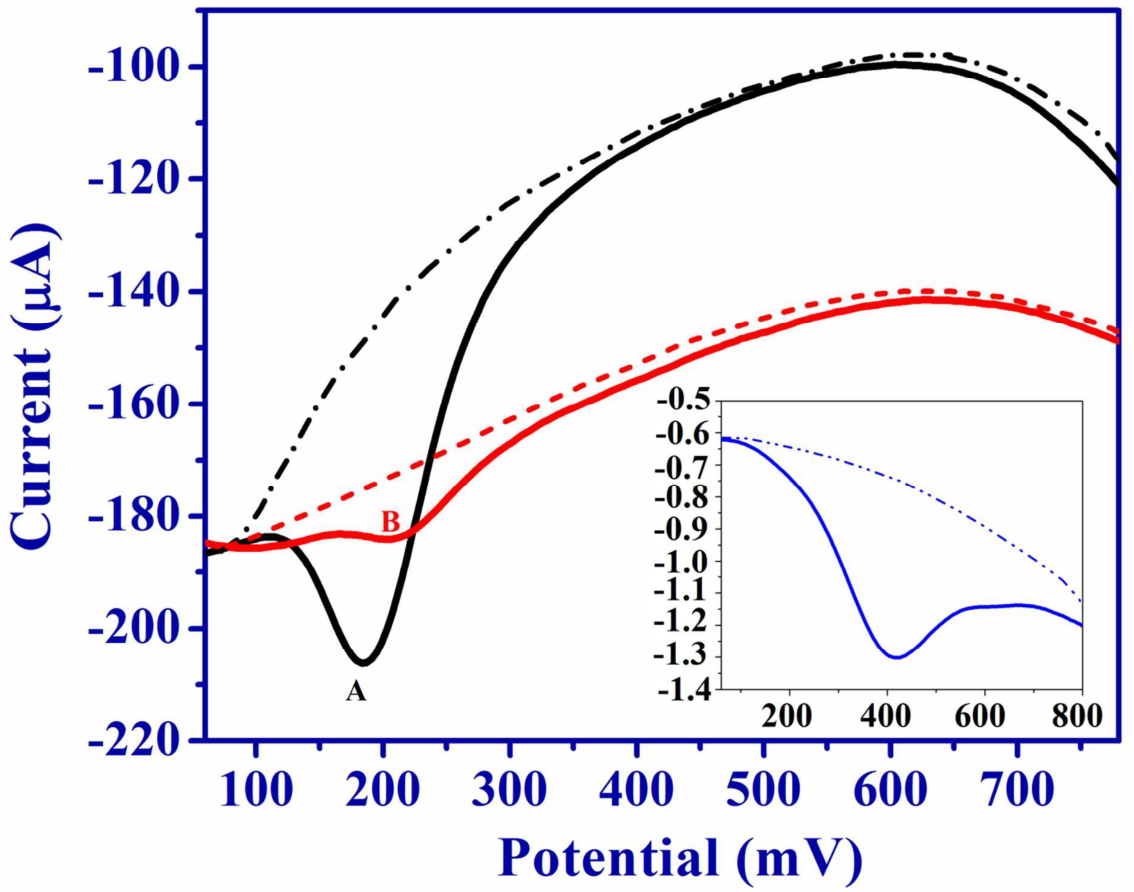
Current (μA)
-100
-120
-140
-160
-180
-200
-220
Potential (mV)
100
200
300
400
500
600
700
A
B
-0.5
-0.6
-0.7
-0.8
-0.9
-1.0
-1.1
-1.2
-1.3
-1.4
200
400
600
800

Figure 5

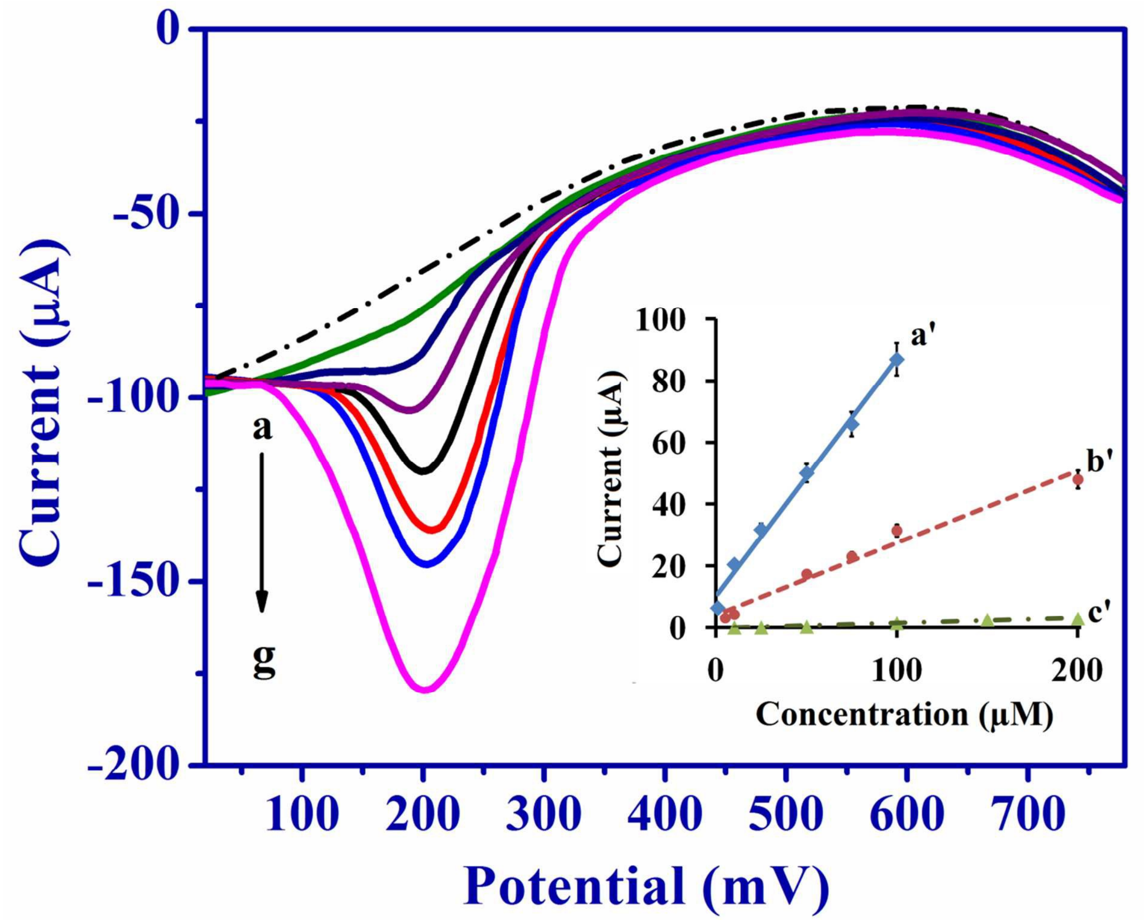
0
-50
-100
-150
-200
Current (μA)
100
200
300
400
500
600
700
Potential (mV)
a
g
100
80
60
40
20
0
Current (μA)
0
100
200
Concentration (μM)
a'
b'
c'

Figure 6

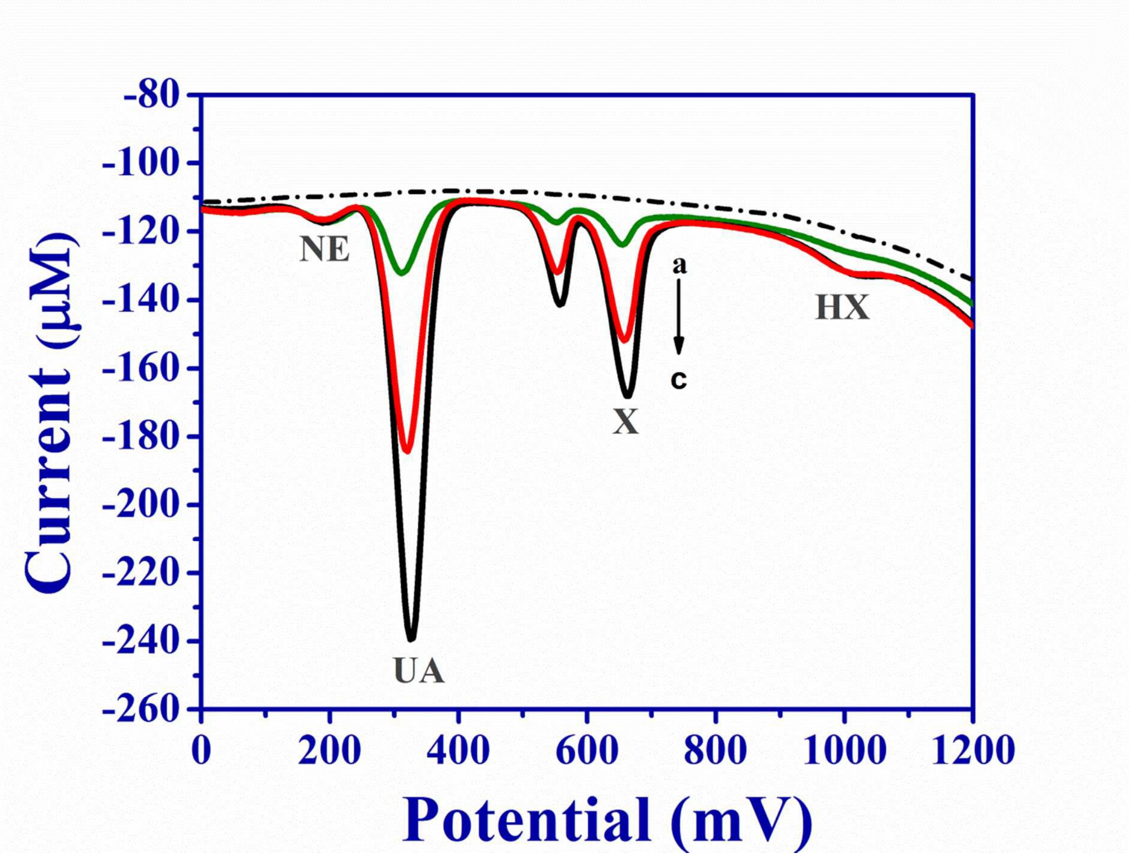
Current (µM)
-80
-100
-120
-140
-160
-180
-200
-220
-240
-260
Potential (mV)
0
200
400
600
800
1000
1200
NE
UA
X
HX
a
c

Figure 7